Dual-band Bandpass Double Ground Plane Coaxial Resonators and Filters

Dual-band Bandpass Double Ground Plane Coaxial Resonators and Filters

Efstratios Doumanis, *Member, IEEE*, Lei Guan, *Member, IEEE*, George Goussetis, *Senior Member, IEEE*, and Dieter Ferling

***Abstract*—This contribution proposes a novel double ground plane coaxial resonator that allows to utilize two independent coaxial cavity modes in reduced physical volume. This configuration of compact high performance filters is an enabler for multi-band transmitter architectures using modern Radio Frequency data convertors (RFDAC). The benefit of the proposed approach is the ease of design and the design flexibility. The filters proposed, provide the ability to control the frequency, the bandwidth and the introduction of transmission zeroes (TZs) separately for each band. A number of designs are presented to demonstrate the operation principle and the performance characteristics of the proposed filters. A 2x4 pole filter has been manufactured and tested with very good obtained results.**

***Index Terms*— base transceiver station, BTS, coaxial, dual-band, filters, fifth generation (5G), long-term evolution (LTE), mass-production, resonators .**

I. Introduction

To provide extreme better-than-ever wireless network user experience, modern wireless communications systems, e.g., the forthcoming fifth generation (5G) wireless systems are heading for larger network capacity with higher data-rate wireless access. However, frequency spectrum, as the only medium of information carrier for wireless communications, is getting more-than-ever crowded, especially below 6 GHz. It is very difficult for any wireless network operator to occupy a large continuous frequency spectrum, leading to frequency fragment situation in general. Two very popular and effective approaches have been explored both in academia and industry for better utilization of frequency spectrum including 1) large scale antenna systems [1], which replace the conventional simple antenna array (smaller than 16 radiating elements) by a bigger active antenna array (greater than 60 radiating elements) to significantly increase the spectrum utilization efficiency by spatial multiplexing at cost of extra digital horse-power [2] and 2) carrier aggregation, which directly utilizes multiple frequency bands simultaneously to create a virtualized wideband channel serving end users with higher data rates at cost of affordable engineering efforts. From end-user point of view, wider-band carrier aggregation transmission will proportionally and directly increase the data rates leading to better user experience.

Due to the physical limitation (such as sampling rate of the data convertors (DACs)), the conventional carrier aggregation schemes transmit multi-band signals via multiple RF chains at the basestation side and combine the multi-band signals at the user receiver side. The emerging RF-class data convertors, e.g., RFDAC and RFADC (at a couple of Giga Symbols per Second -GSPS) enables a very compact single-chain multi-band radio transmitter solution. Fig. 1 illustrates both conventional multi-chain multi-band radio and compact single-chain multi-band radio. By utilizing RFDAC, wideband / multi-band power amplifiers (MBPA), two-port multi-band filters and wideband antennas, this new radio architecture significantly reduces the number of both active and passive analog components, making it a very attractive compact multi-band radio solution for base-stations with inherent almost-perfect synchronization between multiple frequency bands in a dense deployment scenario.

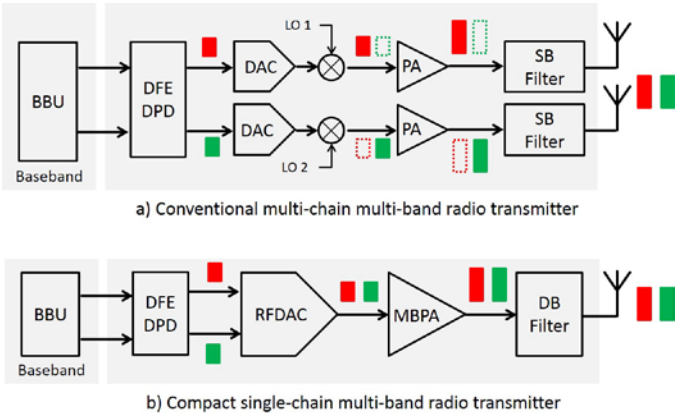

Fig. 1. Simplified diagrams of multi-band radio transmitters at wireless base-stations (using two bands as an example).

Besides the challenges of multi-band RF signal conditioning algorithms, like digital predistortion (DPD) and crest factor reduction (CFR) for wideband/multi-band PA realized in the digital frontend (DFE), a new architecture and implementation of two-port multi-band cavity filters is essential as indicated in the Fig. 1 for creating this compact

Manuscript received July 25th, 2017.

E. Doumanis, and L. Guan, are with Nokia Bell Laboratories, Dublin, Ireland (e-mail: efstratios.doumanis, lei.guan@nokia-bell-labs.com).

G. Goussetis is with the Sensors, Signals and Systems, School of Engineering and Physical Sciences, Heriot Watt University, Edinburgh, UK (e-mail: g.goussetis@hw.ac.uk).

D. Ferling, is with Nokia Bell Laboratories, Stuttgart. Germany (e-mail: dieter.ferling@nokia-bell-labs.com).

single-chain multi-band radio transmitter. Dual-band filters [3] - [34] represent an attractive solution to reduce the overall number of passive elements and cost for multiband high performance radio remote heads (RRHs). There are various techniques and approaches in the design, synthesis and implementation of dual-band filters [3]-[12]. Dual-band filters have been implemented in many different technologies, such as, planar [13]-[19], waveguide [20]-[22], combline [23]-[27], helical [28], dielectric resonator [29]-[31], substrate integrated waveguide [32] and low-temperature cofired ceramic (LTCC) technology [33], just to name a few. A signal interference approach in multi-band is investigated in [34].

Among the various implementations, combline technology represents an attractive solution for BTS applications [35]-[39] as it provides advantageous tradeoff in terms of insertion loss (quality factor), power handling and volume. The coaxial cavity resonator technology offers mass-production, low-cost with high technological maturity. Additionally, it offers a wide tuning range and wide spurious-free stopband. Recently a solution involving triple-conductor combline resonators has been proposed and its application in dual-band filters for BTS has been demonstrated [25]. It provides significant size reduction at the expense of reduced flexibility.

This contribution demonstrates a novel configuration for a dual-band coaxial resonator where two cavities are interlaced with the use of an intermediate wall. It allows for independent design of the two modes and provides the building block for dual-band filters for BTS. By means of design examples, we demonstrate the ease of design of filters with these resonators. This contribution is structured as following: Section II describes the physical configuration and the operation principle of the proposed resonator, Section III, describes the utilization of the dual-band resonator to demonstrate the technique to excite the resonators and to couple them. It shows additionally a number of the filter designs. In Section IV experimental results are presented and compared with simulated, while Section V concludes the paper.

II. Double-Ground Plane Resonator

Fig. 2 depicts a sketch of the proposed double coaxial resonator. With view of Fig. 2, the proposed resonator consists of a housing enclosure and an intermediate horizontal wall. This horizontal wall divides the housing enclosure into two electrically isolated cavities which are utilized to create two coaxial resonators. In the cavity at the lower end of the housing, a post is introduced. The intermediate horizontal wall serves as the open end of the lower cavity and also as the post for the upper cavity. Thus, the intermediate wall is simultaneously the top lid for the lower cavity and the ground plane and post for the upper cavity. For the lower cavity, the intermediate horizontal wall is the capacitive loading of the resonator post whereas for the upper cavity the wall represents the post.

The operation principle of the resonator is demonstrated in Fig. 3 where the field distribution of the two modes supported by the structure are given. The field distributions indicate the complete electrical isolation between the two modes. Figure 3a and 3b show the magnitude of the electric field distribution of mode 1 and mode 2 respectively, on a two-dimensional surface at a cross section in the middle of the cavity. Accordingly, Fig. 3c and 3d show the magnitude of the magnetic field distribution of mode 1 and mode 2, respectively.

TABLE I
Resonator and Filter Dimensions

Symbol	Quantity	mm
w	cavity width	30
h	cavity height	20.98
h_1	inner cavity height, m1	8
h_2	inner cavity height, m2	11.98
lp_2	post length, m1	15.02
lp_2	post length, m2	9.5
d_1	post diameter, m1	7
d_2	post diameter, m2	13
wt	inner wall thickness	1

For mode 1 resonator, the current configuration allows for increased volume to store magnetic energy at resonance. The mode 1 resonator can be considered as a capacitively loaded combline resonator or equivalently a stepped impedance resonator. Furthermore, it allows the mode 1 resonant mode to couple magnetically to neighboring mode 1 resonators The opening at the bottom for the two mode 1 resonators can provide adequate coupling between them. Comparing the Q-facotr between the conventional resonator and the proposed resonator (the proposed resonator operating at -14.49 % frequency drop) the volume reduction is 48.55 %. The Q/Vol of the conventional resonator is decreased by 18.03 %. Comparing the proposed resonator with the conventional resonator (at the same frequency) there is around 58 % less volume, and the Q/Volume of the conventional resonator is less by 35.39 %. The Q/Volume improvement is due to the capacitive loading of the proposed resonator.

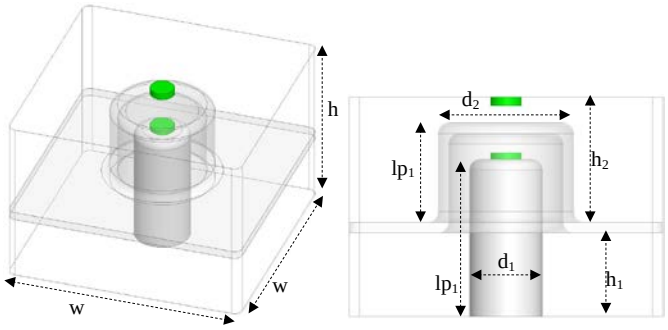

Fig. 2. Computer aided design (CAD) model (Ansys High Frequency Structure Simulator HFSS) of a double-ground plane resonator. The dual-band resonator is operating at mode 1 frequency of 2600 MHz and mode 2 frequency of 3500 MHz. The cylinders at the top of the upper cavity and at the top of the lower resonator post represent tuning screws. The dimensions are given in Table 1.

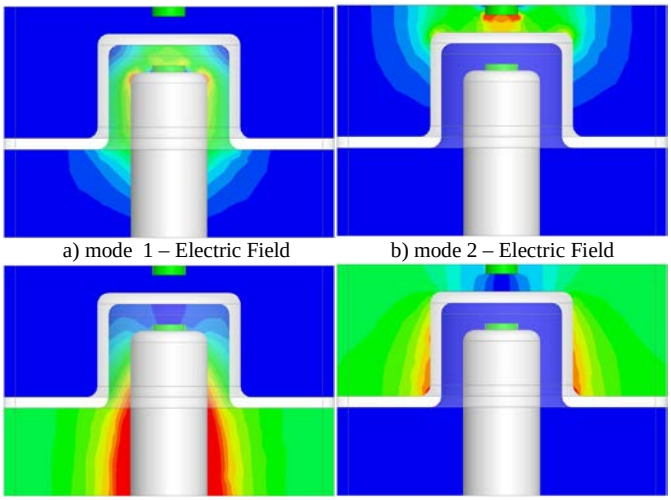

a) mode 1 – Electric Field b) mode 2 – Electric Field

c) mode 1 – Magnetic Field d) mode 2 – Magnetic Field

Fig. 3. Operation principle of the dual-band resonator. Electric field at resonant frequency of a) mode 1 and b) mode 2. Magnetic field at resonant frequency for c) mode 1 and d) mode 2. Mode 1 resonant frequency is 2600 MHz and mode 2 resonant frequency is 3500 MHz. Intense color represents the higher intensity and less intense color represents lower intensity.

The mode 2 resonator differs from the conventional coaxial resonator only in the ratio of the diameter of the post to the diameter of the external cavity. In the proposed resonator the diameter of the post is larger than the conventional resonator diameter. The resonator post is also hollow that allows extra volume for the mode 1 resonator. The fact that the mode 2 conductor can have a large diameter, the area between the top lid and the mode 2 post allows for a large volume to store electric energy resembling hat resonators which in turn, with regards to the Q-factor, compensates for the non-optimum diameter and allows for efficient resonators. A study is performed (not included for brevity) that calculates the Q-factor and resonant frequency of the proposed upper cavity resonator as a function of the resonator post diameter. The two extremes of the study show two cases that represent the traditional post diameter to cavity diameter ratio (0.3) and one example resonator with wider ratio (0.46). With 15.4 % less physical volume, at a 6.47 % lower frequency, the proposed resonator with a ratio of 0.46 demonstrates a Q/Vol increase by around 5 %. Assuming that the frequency is then matched then this means that the benefit will increase.

The design of the proposed resonator is similar to the design of the conventional coaxial cavity resonator. In particular, the optimization of the performance of the resonators is dependent of the frequency ratio between the two modes.

In relation to selecting the dimensions of the cavities, as in the conventional case this is performed in light of the Q-factor requirements. In particular, the resonator with the higher Q-factor requirement will determine the footprint of the dual-band resonator. The bottom resonator is preferable operating at a lower frequency. Due to the lower frequency of operation, it requires more physical volume for the same performance. Once the footprint for the top or bottom resonator is determined, then the remaining parameters follow. The diameter of the post of the bottom resonator is determined with the same guidelines, and then the diameter of the top resonator hollow post needs to be adjusted to accommodate for the post of the bottom resonator. The electrical length of the resonator is similar to the electrical length of the conventional resonator that is capacitively loaded. The frequency can be tuned by adjusting the gap between the open end of the resonator and the lid. The respective lengths of the two posts are finally determined to fix the two frequency bands. The fine tuning of the resonator parameters requires further full-wave optimization. The above procedure provides first dimensions for the resonators.

The synthesis process also needs to be adjusted to the proposed structure. Firstly, we note that given that the responses associated with the top and bottom resonators are virtually independent, the synthesis of the two bands in terms of the coupling matrix can take place independently. The standard procedure can then be applied for each band; for I/O coupling, we have proposed to use taping for the lower resonator and inductive coupling for the top resonator. The group delay technique can again be used in order to achieve the required external Q-factor. The coupling coefficient between the resonators is controlled by the inductive irises. A main factor to take into account is the frequency ratio of the two bands (f_2/f_1). This configuration provides the ability to independently control the two bands, in terms of center frequency, bandwidth and the introduction of TZs separately for each band. A benefit of this configuration is the high levels of isolation between the two frequency bands with a minimum sacrifice in the overall Q-factor. It is noted that since the lower and upper cavities are electrically isolated, the tuning of the two resonances, can now be almost independent as compared to prior art. In this case, the post fabrication tuning efforts can significantly reduce the overall design complexity. This allows to reduce the design complexity of radio band (RB) filters for real-life BTS filters. In summary, this technology offers ease of design and high flexibility with high performance.

A benefit of the proposed solution comes from improving the physical configuration to allow transmission zeros, which are of pertinent importance in efficient base station (BS) filters. Furthermore, the implementation of the transmission zeros is feasible in the conventional way (by cross-couplings), and can be implemented for TZs both in the upper and lower stopbands of the two passbands of the filter. This gives increased flexibility of the proposed solution.

III. Coupling and Filter Design

A. *External Coupling*

pd_1

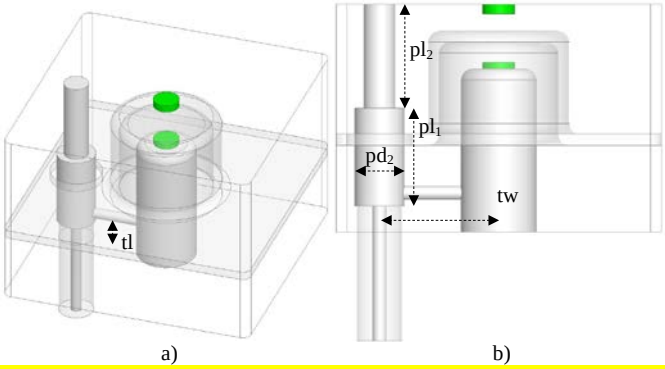

Fig. 4. CAD model (Ansys HFSS) of a double-ground plane resonator with the excitation method employed. The dimensions of the resonator are that of Fig. 2.

The excitation methods of a standard combline resonator and of conventional diplexers can also be readily applied to this resonator. One common method involves the inner conductor of a coaxial line (SubMiniature version A-SMA connector) being tapped into the resonator post; adjusting the height of the tapping establishes a suitable impedance for the excitation. An alternate excitation method isis also considered [40]Themethod includes a metallic post protruding the cavity from the bottom wall extending to the top wall where it is grounded. The inner conductor of a coaxial line (SMA connector) is tapped into the bottom end of the metallic post. The excitation methods are combined and are employed for the excitation of the resonators and the filters. Fig. 4 shows a CAD model of the dual-band resonator. Suitable excitation for mode 1 is established by adjusting the height of the tapping pin to the mode 1 post. Likewise, suitable excitation for mode 2, is established by adjusting the location and distance of the metallic post to the center conductor of the resonator. A wide range of external coupling bandwidths can be achieved by this excitation technique similar to the excitation techniques of single-band resonators. Fig. 5a show the calculated S-parameters at the excitation port of the dual-band resonator of Fig. 4. It clearly shows the two dips in the S_{11} demonstrating the two resonant frequencies of the structure. Accordingly, fig. 5b shows the group delay at the excitation port.

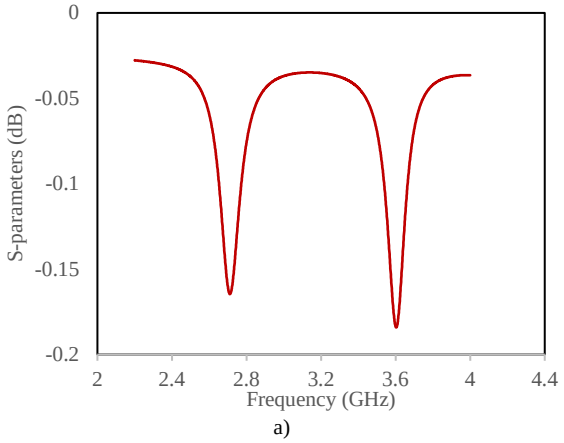

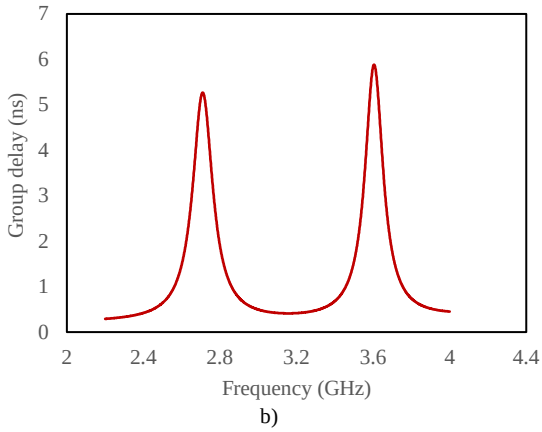

Fig. 5. S-parameters a) and group delay b) of a dual-band resonator of Fig. 4. Dims (mm): pd_1=2.9, pd_2=4.6, pl_1=9, pl_2=9.98, tl=3.6 tw=11.

B. *Inter-resonator Coupling*

The inter-stage coupling between adjacent resonators follows the same principles as conventional coaxial combline resonators. Common slots across the entire length of the resonator are employed for both the first and the second modes (lower and upper cavities). For the first mode, the coupling is predominantly inductive and there is very little capacitive contribution at the open end of the coupled resonators as opposed to the conventional case. This is due to the concentration of the electric field in the inner part of the intermediate wall. For the second mode, the coupling is again predominantly magnetic but in this case the coupling has the capacitive contribution more pronounced compared to the first mode, as in the conventional case. By utilizing an iris along the width of the cavity (see Fig. 7), the two couplings, magnetic and electric, coexist and cancel each other since they are opposite in phase. The coupling of non-adjacent resonators can be both of inductive (through a slot at any side of the cavity, bottom or top) and capacitive (through the commonly used technique of a capacitive probe). In the conventional coaxial resonator coupling with an inductive iris with an opening at the bottom end of the resonators where the posts are grounded, the inductive coupling reaches a maximum value once the opening is approximately forty percent of the total height of the resonator cavity [37],. Thus, in the proposed lower cavity resonator, allowing some height before the capacitive wall enclosure, one can allow to achieve even the maximum of coupling. To demonstrate the coupling between two dual-band resonators, Fig. 6 shows the calculated coupling coefficients for both modes as a function of the width of the intermediate iris opening. The coupling coefficient of mode 1 is represented by the solid black curve and it shows an increase from a small value to a quite high value as the iris is as wide as almost the entire width of the cavity. Similar results are shown for the case of mode 2 where the coupling is increased as the width of the iris opening is increased. The capacitive contribution is introduced at all the iris' widths. The capacitive contribution would also depend on the capacitive loading at the open end of the resonator. The coupling is quite strong and this is attributed to the greater diameter of the upper resonator posts.

The final configuration of the filter is defined by full-wave optimization. The tuning screws employed for post-fabrication tuning of the coupling can be employed as usual.

C. Frequency Ratio

A dual-band filter requires two separate passbands while providing rejection in a guard band in between the two passbands. The upper limit of the frequency ratio is restricted by the spurious harmonic resonances of the lower resonators (see Fig. 14). The lower limit is effectively restricted at the point where the guard band is significantly reduced in comparison with the passbands. In this respect, this lower limit of this ratio is dependent not only on the centre operating frequencies of the filters but also on the bandwidth associated with each band as well as the skirt selectivity. The number of poles on each band of the dual-band filters determines the intra-band rejection levels of the filters. In practice, the dual-band filters are required to fulfil two distinct frequency bands of 4G and 5G cellular systems. The dual-band filter here is focused on two frequency bands. The lower frequency band is long-term evolution (LTE) frequency division duplexing (FDD) downlink (DL) band 7 (LTE FDD Band 7 DL: 2620-2690 MHz) and the higher frequency band is LTE FDD DL band 22 (LTE FDD Band 22 DL: 3510-3590 MHz). The physical dimensions in the manuscript are not adopted on a strict performance criteria, but as a study unit with some mechanical dimensions required to ease the design and the fabrication and handling of the prototypes. Thus, they represent not fully optimized resonators.

D. 2x2 Pole Filter Design

This section shows the design of filters based on the proposed dual-band resonators and presents design examples. The design of the filters follows the conventional design of the coaxial filters, starting with the design of the individual resonator. The design of the individual filters follows the conventional design. Fig. 7 shows the CAD model of 2x2 pole filter. The excitation of the previous section is employed at the input and output resonators. The coupling irises are employed to couple the mode 1 and mode 2 resonators. Tuning screws are required to fine-tune the frequency of the two modes. Fig. 9 (solid line) shows the obtained S-parameters of the 2x2 pole filter of Fig. 7. The rejection levels at the lower and upper stopbands of the filters are relevant to the order of the filter.

E. 2x4 Pole Filter Design

Fig. 8 shows a CAD model of a 2x4 pole filter. Each band has 4 poles that are arranged in a folded configuration. Fig. 9 shows the obtained results of the filter (dashed lines). The two bands are the same as the previous example. Fig. 9, shows the comparison of the simulated results of the 2x2 pole filter vs. the 2x4 pole filter and demonstrates the rejection levels improvement with the number of poles of each filter. It is demonstrated that the isolation levels between the two bands is almost -80 dB and can be improved with the order of the filters as shown in this example.

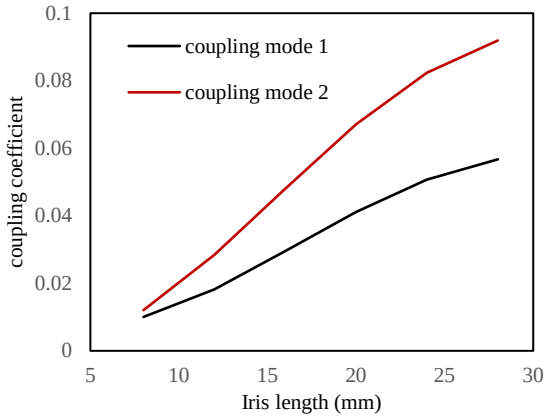

Fig. 6. Calculated coupling coefficient for the two modes as a function of the iris length for mode 1 and mode 2.

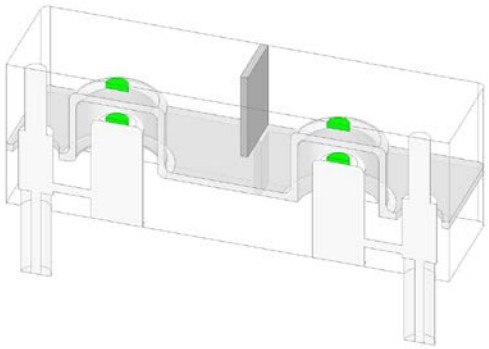

Fig. 7. CAD model of the 2x2 pole filter. The figure shows half of the filter. The green elements represent the tuning elements.

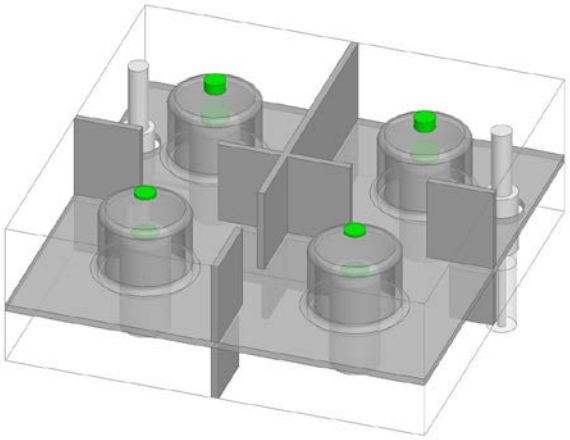

Fig. 8. CAD model of a 2x4 pole filter. Each band has 4 poles that are arranged in a folded configuration.

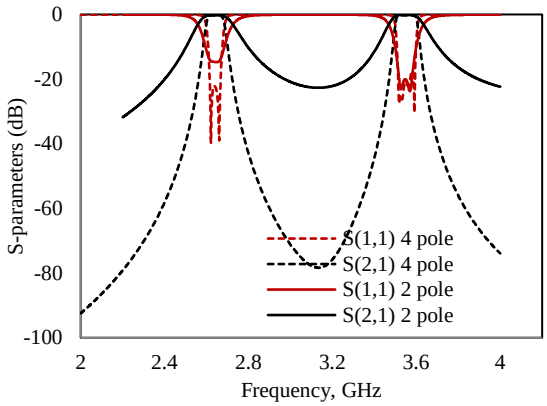

Fig. 9. Simulated 2x2 pole (solid lines) and 2x4 pole (dashed lines) filters superimposed for comparison.

IV. Experimental Results

The 2x4 pole design of the previous example has been fabricated and tested. Fig. 10 shows the fabricated prototype. The prototype was fabricated in Aluminum. It consists of 3 pieces, the top lid, the intermediate wall and the bottom cover. Fig. 10b shows the top surface of the intermediate wall. This piece has been made out of one single block of material that has been machined both sides. The thickness of the wall is 1 mm. The bottom piece is also shown in Fig. 10c. The internal dimensions of the filter are: 60x60x21 mm^3. Fig. 11a shows the measured response of the 2x4 dual-band filter. The simulated response is superimposed for comparison. The measured results compare very well with the simulations. There is a slight frequency shift in both of the bands. In the low frequency band the measured frequency shift is around 13 MHz lower whereas in the high frequency band the measured shift is around 16 MHz representing a shift of smaller than 0.5 % in both cases. The minor discrepancies are attributed to mechanical inaccuracies and small deviations of the simulated model to the fabricated filter. There is a minor discrepancy in the out-of-band performance of the dual-band filter. In particular, the out-of-band rejection levels in the intermediate frequency band are approximately 73 dB whereas the simulated value is around 77 dB. This is attributed to the frequency shift in both bands. This frequency shift affects the out-of-band performance of the dual-band filter in between the two bands. These discrepancies are attributed to the excitation inaccuracies.

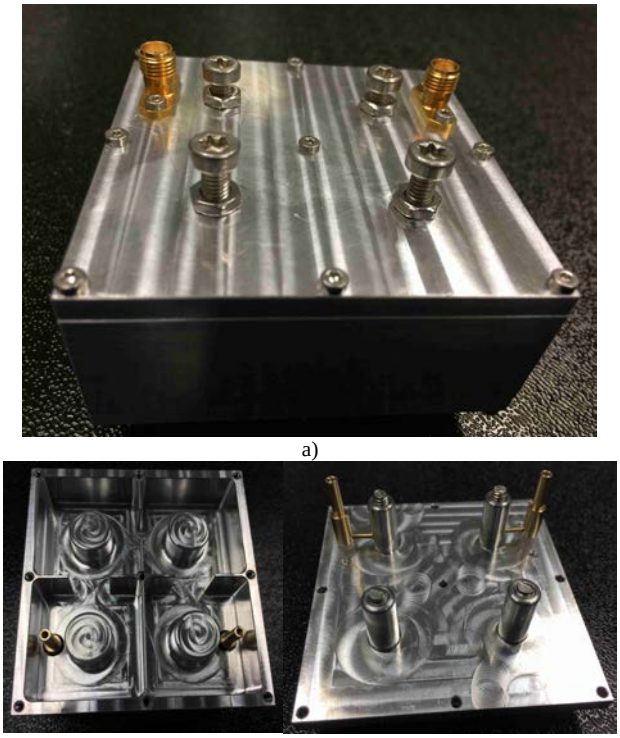

Fig. 10. Photographs of the fabricated prototype 2x4 pole filter. The photographs, show the assembled filter, the intermediate piece and the bottom cover. The filter has been machined in Aluminum and then silver-plated.

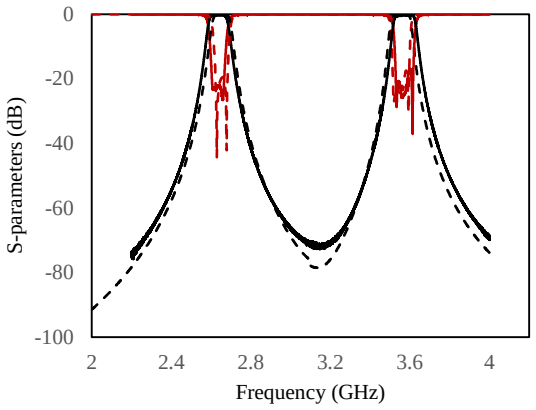

Fig. 11. Measured (solid line) 2x4 pole filter response, simulated results (dashed line) superimposed for comparison.

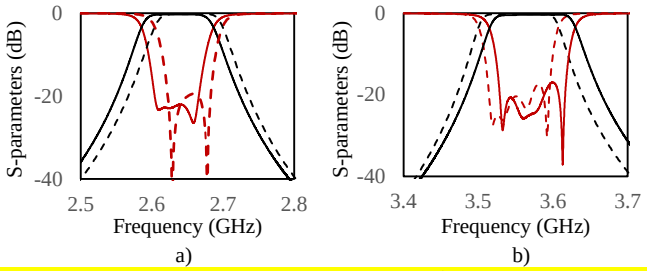

Fig. 12. In-band measured (solid line) 2x4 pole filter response, simulated results (dashed line) superimposed for comparison, a) lower frequency band, b) higher frequency band.

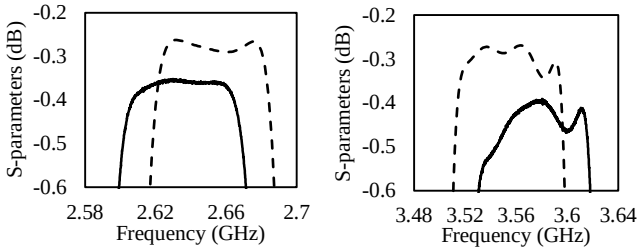

Fig. 13. In-band measured (solid line) 2x4 pole filter response – insertion loss, simulated results (dashed line) superimposed for comparison, a) lower frequency band, b) higher frequency band.

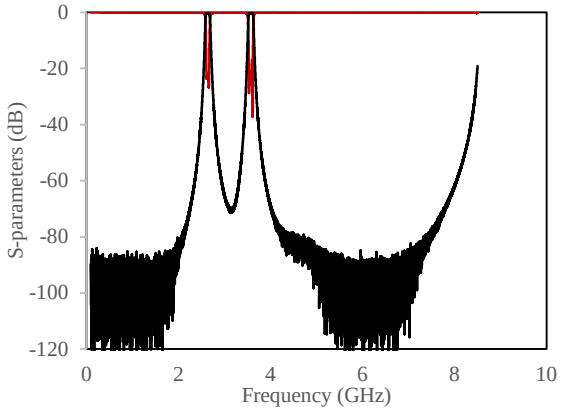

Fig. 14. Measured wideband response of the 2x4 pole filter.

Fig. 12a and Fig. 12b, show the in-band performance of the two frequency bands of the filter. It is demonstrated that in both frequency bands, the filter is well-matched at both bands, the filter return loss levels are below -20 dB for the lower frequency band and smaller than -17.5 dB for the higher frequency band. Fig. 13a and Fig. 13b show the in-band insertion loss of the filter at the two frequency bands. The simulated insertion loss of the low frequency band is ~0.28 dB whereas the measured insertion loss is ~0.34 dB. The simulated insertion loss of the high frequency band is ~0.28 dB whereas the measured insertion loss is ~0.39 dB. The results in terms of the insertion loss are in excellent agreement. The minor discrepancy is attributed to the surface roughness. Fig. 14 shows the broadband response of the filter and demonstrates the first harmonic output of the filter. The first harmonic appears at around 9 GHz in line with simulations and represents the harmonic output of the mode 1 filter. The harmonic output is approximately 3.2 times the resonant frequency of the first mode.

V. Conclusion

A simple and efficient technique to implement dual-band filters in coaxial cavity technology is demonstrated. The easy of design and implementation along with the compactness of the proposed solution are the main benefits. A 2x4 pole filter has been designed, manufactured and tested with very good obtained results.

References

[1] T.L. Marzetta, “Massive MIMO: an introduction,” *Bell Labs Technical Journal*, vol. 20, pp. 11-20, Mar. 2015.

[2] L. Guan, FPGA-based Digital Convolution for Wireless Applications Springer Series in Wireless Technology, Springer, 2017.

[3] U. Rosenberg, "Multiplexing and double band filtering with common-multimode cavities," *IEEE Trans. Microw. Theory Techn.*, vol. 38, no. 12, pp. 1862-1871, Dec. 1990.

[4] H. Miyake, S. Kitazawa, T. Ishizaki, T. Yamada, and Y. Nagatomi, "A miniaturized monolithic dual band filter using ceramic lamination technique for dual mode portable telephones," in *Proc. Intern. Microw. Symposium Digest*, 1997, pp. 789-792.

[5] L. -C. Tsai, and C. -W. Hsue, "Dual-band bandpass filters using equal-length coupled-serial-shunted lines and Z-transform technique," *IEEE Trans. Microw. Theory Techn.*, vol. 52, no. 4, pp. 1111-1117, Apr. 2004.

[6] R. J. Cameron, M. Yu, and Y. Wang, “Direct-Coupled microwave filters with single and dual stopbands,” *IEEE Trans. Microw. Theory Techn.*,vol. 53, no. 11, pp. 3288-3297, Nov. 2005.

[7] G. Macchiarella, S. Tamiazzo, "Design techniques for dual-passband filters," *IEEE Trans. Microw. Theory Techn.*, vol. 53, no. 11, pp. 3265-3271, Nov. 2005.

[8] P. Lenoir, S. Bila, F. Seyfert, D. Baillargeat, S. Verdeyme, "Synthesis and design of asymmetrical dual-band bandpass filters based on equivalent network simplification," *IEEE Trans. Microw. Theory Techn.*, vol. 54, no. 7, pp. 3090-3097, Jul. 2006.

[9] M. Mokhtaari, J. Bornemann, K. Rambabu, S. Amari, "Coupling-matrix design of dual and triple passband filters," *IEEE Trans. Microw. Theory Techn.*, vol. 54, no. 11, pp. 3940-3945, Nov. 2006.

[10] C.-Y. Chen, and C.-Y. Hsu, "A simple and effective method for microstrip dual-band filters design," *IEEE Microw. & Wirel. Comp. Let.*, vol. 16, no. 5, pp. 246-248, May 2006.

[11] J. Lee, K. Sarabandi, "A synthesis method for dual-passband microwave filters," *IEEE Trans. Microw. Theory Techn.*, vol. 55, no. 6, pp. 1163-1170, Jun. 2007.

[12] V. Lunot, S. Bila, F. Seyfert, "Optimal synthesis for multi-band microwave filters," in *IEEE MTT-S Int. Microw. Symp. Dig.*, 2007, pp. 115-118.

[13] H.-M. Lee, C.-R. Chen, C.-C. Tsai, and C-M.Tsai, "Dual-band coupling and feed structure for microstrip filter design" in *IEEE MTT-S Int. Microw. Symp. Dig.*, vol. 3, 2004, pp. 1971-1974.

[14] H.-M. Lee, C.-M. Tsai, and C.-C. Tsai, "Transmission-line filter design with fully controllable second passband," in *IEEE MTT-S Int. Microw. Symp. Dig.*, vol. 4, 2005, pp. 2191-2194.

[15] J.-T. Kuo, T.-H. Yeh, and C.-C. Yeh, "Design of microstrip bandpass filters with a dual-passband response," *IEEE Trans. Microw. Theory Techn.*, vol. 53, no. 4, pp. 1331-1337, Apr. 2005.

[16] C-F. Chen, T.-Y. Huang, and R.-B. Wu, "Design of dual-and triple-passband filters using alternately cascaded multiband resonators," *IEEE Trans. Microw. Theory Techn.*, vol. 54, no. 9, pp. 3550-3558, Sep. 2006.

[17] X. Y. Zhang, J.-X. Chen, Q. Xue, and S.-M. Li, "Dual-band bandpass filters using stub-loaded resonators," *IEEE Microw. Wirel. Comp. Lett.*, vol. 17, no. 8, pp. 583-585, Aug. 2007.

[18] X. Y. Zhang, C. H. Chan, Q. Xue, and B-J. Hu, "Dual-band bandpass filter with controllable bandwidths using two coupling paths," *IEEE Microw. Wirel. Comp. Lett.*, vol. 20, no. 11, pp. 616-618, Nov. 2010.

[19] S. Fu, B. Wu, J. Chen, S-J. Sun, and C-H. Liang, "Novel second-order dual-mode dual-band filters using capacitance loaded square loop resonator," *IEEE Trans. Microw. Theory Techn.*, vol. 60, no. 3, pp. 477-483, Mar. 2012.

[20] S. Amari, M. Bekheit, "A new class of dual-mode dual-band waveguide filters," *IEEE Trans. Microw. Theory Techn.*, vol. 56, no. 8, pp. 1938-1944, Aug. 2008.

[21] M. M. Fahmi, J. A. Ruiz-Cruz, R. R. Mansour, and K. A. Zaki, “Compact wide-band ridge waveguide dual-band filters,” in *IEEE MTT-S Int. Microw. Symp. Dig.*, 2010, pp. 888-891.

[22] U. Naeem, S. Bila, M. Thévenot, T. Monédière, and S. Verdeyme, "A dual-band bandpass filter with widely separated passbands," *IEEE Trans. Microw. Theory Techn.*, vol. 62, no. 3, pp. 450-456, Mar. 2014.

[23] X. Liu, L. P. B. Katehi, and D. Peroulis, "Novel dual-band microwave filter using dual-capacitively-loaded cavity resonators," *IEEE Microw. Wirel. Comp. Lett.*, vol. 20, no. 11, pp. 610-612, Nov. 2010.

[24] A.I. Abunjaileh, I.C. Hunter, “Tunable bandpass and bandstop filters based on dual-band combline Structures,” *IEEE Trans. Microw. Theory Techn.*, vol. 58, no. 12, pp. 3710-3719, Dec. 2010.

[25] J. A. Ruiz-Cruz, M. M. Fahmi, R. R. Mansour, "Triple-conductor combline resonators for dual-band filters with enhanced guard-band selectivity," *IEEE Trans. Microw. Theory Techn.*, vol. 60, no. 12, pp. 3969-3979, Dec. 2012.
[26] F.-C. Chen, J.-M. Qiu, S.-W. Wong, and Q.-X. Chu, "Dual-band coaxial cavity bandpass filter with helical feeding structure and mixed coupling," *IEEE Microw. Wirel. Comp. Lett.*, vol. 25, no. 1, pp. 31-33, Jan. 2015.
[27] A. Perigaud, etal, "Compact dual-band filter in SIW technology for a L band receiver," in *Proc. IEEE European Microw. Conf. (EuMC)*, 2015, pp. 765-768.
[28] Q.-X. Chu, and Z.-C. Zhang, "Dual-band helical filters based on nonuniform pitch helical resonators," *IEEE Trans. Microw. Theory Techn.*, To be published, 2017.
[29] R. Zhang, R. R. Mansour, "Dual-Band dielectric-resonator filters," *IEEE Trans. Microw. Theory Techn.*, vol. 57, no. 7, pp. 1760- 1766, Jul. 2009.
[30] M. Memarian, and R. R. Mansour, "Dual-band half-cut dielectric resonator filters," in *Proc. European Microw. Conf., (EuMC)*, 2009, pp. 555-558.
[31] M. Mohammad, "Novel quadruple-mode, dual-mode and dual-band dielectric resonator filters and multiplexers," M. S. thesis, Electr. And Comp. Eng., Waterloo, Canada, 2009. "ch. 5". Available online: https://uwspace.uwaterloo.ca/handle/10012/4609.
[32] X.-P. Chen, K. Wu, and Z.-L. Li, "Dual-band and triple-band substrate integrated waveguide filters with Chebyshev and quasi-elliptic responses," *IEEE Trans. Microw. Theory Techn.*, vol. 55, no. 12, pp. 2569-2578, Dec. 2007.
[33] B.-J. Chen, T.-M. Shen, R.-B. Wu, "Dual-band vertically stacked laminated waveguide filter design in LTCC technology," *IEEE Trans. Microw. Theory Techn.*, vol. 57, no. 6, pp. 1554-1562, Jun. 2009.
[34] R. Gomez-Garcia, M. Sanchez-Renedo, B. Jarry, J. Lintignat, and B. Barelaud, "A class of microwave transversal signal-interference dual-passband planar filters," *IEEE Microw. & Wirel. Comp. Lett.*, vol. 19, no. 3, pp. 158-160, Mar. 2009.
[35] G. L. Matthaei, "Comb-line band-pass filters of narrow or moderate bandwidth," *Microw. J.*, vol. 6, pp. 82–91, Aug. 1963.
[36] R. J. Wenzel, "Synthesis of combline and capacitively loaded interdigital bandpass filters of arbitrary bandwidth," *IEEE Trans. Microw. Theory Tech.*, vol. 19, no. 8, pp. 678–686, Aug. 1971.
[37] Y. Rong, and K. A. Zaki, "Full-wave analysis of coupling between cylindrical combline resonators," *IEEE Trans. Microw. Theory Techn.*, vol. 47, no. 9, pp. 1721-1729, Sep. 1999.
[38] R. J. Cameron, C. M. Kudsia, and R. R. Mansour, Microwave Filters for Communication Systems Fundamentals, Design, and Applications. New York, NY, USA: Wiley-Interscience, 2007.
[39] R. R. Mansour, "Filter technologies for wireless base stations," *IEEE Microw. Mag.*, vol. 5, pp. 68–74, Mar. 2004.
[40] E. M. Hansmann, "An investigation of coupling mechanisms in narrow-band microwave filters," M.S. thesis, Dept. Elect. Electron. Eng., Univ. Stellenbosch, Stellenbosch, South Africa, 2009.